Bull. ERS, No. 20(1987)

MODEL TEST FOR BUCKLING FAILURES OF CANTILEVERED CYLINDRICAL SHELLS UNDER A TRANSVERSE LOAD

by

H.S.Choi [I)], T.Tanami [I)], S.Ohya [I)] and Y.Hangai [I)]

INTRODUCTION

When cantilevered cylindrical shells such as liquid-storage tanks and containment vessels, etc. are subjected to earthquake excitation or wind load, failures of these shells may be caused mainly by buckling or elephant-foot bulging as shown in actual damages(1). In order to examine the mechanisms of these failures, a lot of tests have been carried out since Lundquist(2).

However, these failures are strongly influenced by many factors, such as geometrical parameters, boundary and loading conditions as well as material properties so that it is very complicate problem to evaluate the failure mechanisms exactly. Then, the present state is not sufficient to compile the design formulas for this problem so that more theoretical and experimental results are needed.

The authors presented results of a part of a series of tests(3), and the purpose of this paper is to describe another part of this series of tests, comparing with the previous experimental results.

SCHEME OF EXPERIMENT

Models and Test Set-up

The cylindrical models were made by wrapping 0.65mm thick mild steel sheets or 1mm thick aluminium sheet around a mandrel and then welding the longitudinal seam. The end of models were welded to 20mm thick steel and aluminium flanges,respectively, to produce clamped edges. The material properties and dimensions of models are given in Tables.1 and 2.

The test set-up was designed as shown in Fig.1 to apply the shearing forces to the upper flange directly by use of an actuator. And the test were carried out under cyclic loading conditions controlled by the prescribed top displacement.

Measurement of Displacement and Strain

The initial imperfection and the displacement of circular section according to the incremental top displacement were measured by rotating device along the circumference direction, as shown in Fig.2. The strains are mainly measured for the portions subjected to the maximum shearing stress and compressive stress by the strain gauges attached on the inside and outside surface.

I) Institute of Industrial Science, University of Tokyo.

EXPERIMENTAL RESULTS

Material Tests

The stress-strain curves of materials obtained by the uniaxial tensile tests for the steel and aluminium specimens are shown in Fig.3 and 4, respectively. And the mechanical properties of material are given in Table.2.

Load-Displacement Curves

The load-top displacement curves for Models IV-S2,IV-S3,IV-S4 and IV-A3 obtained by the cyclic transverse loading are shown in Fig.5-7 and 8, respectively. The failure mechanisms of IV-S2,IV-S3 and IV-A3 occured in the elasto-plastic region were local
(bending) buckling, while IV-S4 showed elasto-plastic shear buckling. These buckling phenomenon decreased the stiffness of models acutely and occured at twice according to the cyclic loading
direction of plus and minus at the maximum load.

Measured Results of Strains

The strain levels of models at the onset of buckling showed the elasto-plastic region of material, after the buckling, it have progressed in the plastic region as shown in Fig.9. In this paper, authers showed a load-strain curve of IV-A3 for the portion having maximum compressive stress to show the state of progress of strain as an example.

Buckling Mode

The local buckling mode and shear buckling mode for IV-A3 and IV-S4 are shown in Figs.10 and 11, respectively. In Fig.10, each circle from the outside corresponds to the sectional displacement of the height of 0.05L through 0.2L. And each circle corresponds to the sectional displacement of the height of 0.1L through 0.8L in Fig.11.

EVALUATION OF CRITICAL LOAD

Shear Buckling

The test results for the shear buckling are compared with the approximate solution of torsional buckling by Gerard(4). In the case of torsion, the critical shearing stresses for the elasto-plastic buckling, $(\tau)_{cr}$ can be obtain from

$$(\tau_T)_{cr} = 0.701(1-\nu_e^2)^{-0.625} E (t/a)^{1.25} (a/L)^{0.5} \quad (1)$$

$$\eta_p = [(1-\nu_e^2)/(1-\nu^2)]^{0.625} (E_s/E) \quad (2)$$

$$(\tau_p)_{cr} = \eta_p (\tau_T)_{cr} \quad (3)$$

where ν_e, ν =0.5; Poisson's ratio of the elastic region and elasto-plastic region, Es ; secant modulus, $(\tau)cr$; elastic critical shearing stress under torsion and ηp; plastic reduction coefficient. The values of secant modulus was determined by using the test results for the buckling load and it can be obtained from

$$\tau_{cr.exp} = P_{cr.exp} / \pi at \tag{4}$$

$$\sigma_i = \sqrt{3}\ \tau_{cr.exp} \tag{5}$$

where σi ; equivalent stress by von Mises criterion. The results of calculation are shown in Table.3. The comparison of the test results and the approximate values based on the torsional buckling for the critical shearing stress showed good agreement.

Local(Bending) Buckling

The critical loads(Pcr.exp) and the levels of maximum compressive stresses(σcr.exp) of Models IV-S2,IV-S3 and IV-A3 failed by local(bending) buckling are given in Table.4, in which the stress, σcr.exp is obtained from $\sigma cr.exp = Pcr.exp\ L/\pi a^2$.

In this case, the critical stresses were within the range of 35%-49% for the classical buckling stress of uniformly axial compression. However, these models showed the elasto-plastic failure mechanisms, let us compare the critical stresses to the classical buckling stress adapted the plastic reduction coefficient by Krivetsky(5). The plastic reduction coefficient, ηp, can be obtained from Ref.5 by using Es,Et corresponding to the equivalent stress(σi), where Et; tangent modulus, $\sigma i = \sigma cr.exp$. The critical stresses of experiment showed the range of 78%-120% for the approximate value adapted the plastic reduction coefficient as shown in Table.4.

Comparison of Present Results with Other Data

The present results are depicted in Fig.12 by black ovals to compare with the other data. From this figure, it can be seen that there are three regions for (I) elastic local buckling,(II) elastic shear buckling and (III) plastic shear buckling or bulging according to the material properties as well as the geometric parameters. In the figure, the data for (I) were obtained by using vinyl chloride models with the ratios of a/t=250 and 375 in Reference(6). The data for (II) were obtained by three different tests in References(7,8,9) by the use of aluminium(a/t=220), melinex(a/t=200,300,400) and polyester film(a/t=405) models, respectively. In the region(III), two kinds of test results, excepting the present data, are depicted. The first one is the results of steel models with a/t=125,150 and 187, which showed the plastic shear buckling (8). Other tests, which were carried out by steel models of a/t=296 and 395 subjected to internal hydrostatic pressure as well as to transverse shear load, showed the elephant-foot bulging (10). The black circles and white circles for the region IV are showing the previous test data (3) by using the steel models with a/t=150. The dashed and full lines show the numerical results of the elastic shear buckling under transverse shear load(11).

CONCLUSION

The present results indicate:

(a) Local buckling and shear buckling were observed corresponding to the height-to-radius ratio for the steel models with a/t=230 and the aluminium model with a/t=150. These results mean that the failure mechanisms are strongly influenced by the geometric parameters and the material properties by comparing with the present results and previous test data for the steel and aluminium models with a/t=150 failed by the elephant-foot bulging and plastic shear buckling.

(b) The maximum shearing stresses in the case of the elasto-plastic shear buckling were in reasonable agreement with the approximation for the torsional buckling by Gerard.

(c) The critical bending stresses for the local buckling occured in the elasto-plastic region were within about 35%-49% for the classical buckling stress and these values correspond to about 78%-120% for the classical buckling stress of the elasto-plastic region by Krivetsky. The critical stresses are affected by yield stress, Young's modulus and proportional limit stress of materials.

REFERENCES

1) "Greenville(Diablo-Livermore) Earthquake of January 1980: Reconnaissance Report," Earthquake Engineering Research Institute Newsletter, Vol.14, No.2, March 1980, pp.20-89.
2) E.E.Lundquist, "Strength Tests of Thin-Walled Duralumin Cylinders in Combined Transverse Shear and Bending," NACA Technical Note, No.523, 1935.
3) H.S.Choi, et al., "Failure Tests of Cantilevered Cylindrical Shells under a Transverse Load," Proceedings of IASS symposium, Osaka, Vol.1, 1986, pp.265-272.
4) G.Gerard, "Plastic Stability Theory of Thin Shells," Journal of the Aeronautical Sciences, April 1957, pp.269-274.
5) A.Krivetsky, "Plasticity Coefficients for the Plastic Buckling of Plates and Shells," Journal of the Aeronautical Sciences,1955, pp.432-435.
6) K.Uchiyama, et al., "Study on the Buckling of Cylindrical Shells under a Transverse Load," Summaries of Technical Papers of Annual Meeting of AIJ, pp.937-938. (in Japanese)
7) Y.Hangai,et al., "Buckling Failure of Cantilever Type Cylindrical Shells under the Horizontal Load," Bulletine of ERS: University of Tokyo, No.15, pp.13-21.
8) G.D.Galletly, et al., "Buckling of a Cantilevered Cylindrical Shell subjected to a Transverse Shearing Force at its Tip, "Third International Colloquium on Stability of Metal Structures, Paris, November 1983.
9) N.Yamaki, et al., Elastic Stability of Circular Cylindrical Shells, North-Holland, 1984, pp.453-476.
10) H.Okamoto, et al., "Study on the Strength of Cylindrical Tanks for the Earthquake Resistant Capacity," Journal of High Pressure Institute of Japan, Vol.18, No.4, pp.193-199.(in Japanese)
11) P.Schröder, "The Buckling Behaviour of Transverse Loaded Circular Cylinders," Technical Translation ESRO TT-105, 1974.

Table 1. Geometrical Dimensions of Models

Model	Radius a:(mm)	Height L:(mm)	Thickness t:(mm)	L/a	a/t	Material
IV-S2	150	575	0.65	3.83	230	A : Aluminium
IV-S3	150	420	0.65	2.80	230	$E=6.6\times10^5 kg/cm^2$
IV-A3	150	420	1.00	2.80	150	S : Mild Steel
IV-S4	150	275	0.65	1.83	230	$E=2.0\times10^6 kg/cm^2$

IV series : Cyclic Loading

Table 2. Mechanical Properties of Materials

	E (kg/cm^2)	νe	f_p (kg/cm^2)	f_y (kg/cm^2)	f_{max} (kg/cm^2)
Steel	2.0×10^6	0.3	925	2400	3970
Aluminium	6.6×10^5	0.33	1100	1600	2140

f_p : proportional limit stress, f_y : yield stress, f_{max} : failure stress

Table 3. Test Results for Shear Buckling

Model	$P_{cr.exp}$ (kg)	$\tau_{cr.exp}$ (kg/cm^2)	σi (kg/cm^2)	Es (kg/cm^2)	τ_T (kg/cm^2)	ηp	$\tau_{p.cr}$ (kg/cm^2)	$\bar{\tau}$
IV-S4	3100	1012	1752	1.42×10^6	1231	0.795	978	1.03

$\tau_T = (\tau e)cr$, $\bar{\tau} = \tau cr.exp/\tau p.cr$

Table 4. Test Results for Local Buckling

Model	$P_{cr.exp}$ (kg)	σi (kg/cm^2)	Es/E	Et/E	σcl (kg/cm^2)	ηp	$\sigma_{p.cr}$ (kg/cm^2)	$\bar{\sigma}$
IV-S2	1500	1877	0.52	0.23	5243	0.365	1913	0.98
IV-S3	2250	2056	0.51	0.18	5243	0.325	1703	1.20
IV-A3	2200	1307	0.87	0.45	2662	0.625	1663	0.78

$\bar{\sigma} = \sigma cr.exp/\sigma p.cr$, $\sigma i = \sigma cr.exp$

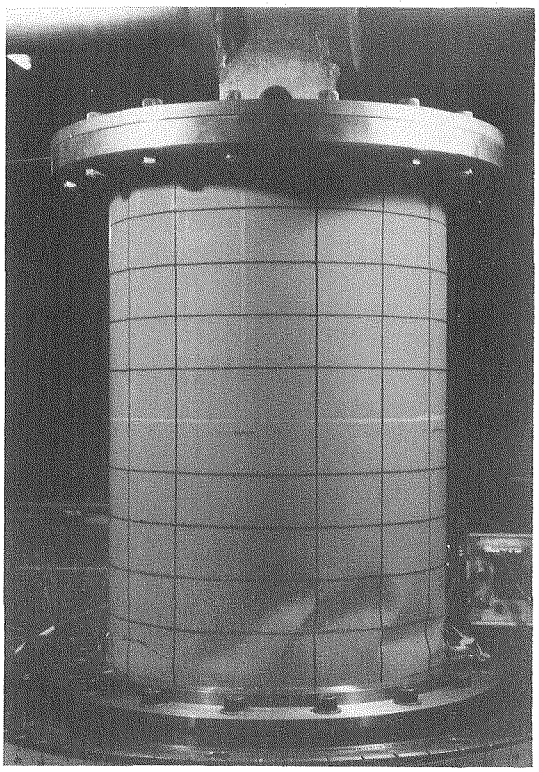

Photo 1. Local Buckling Mode (IV-A3)

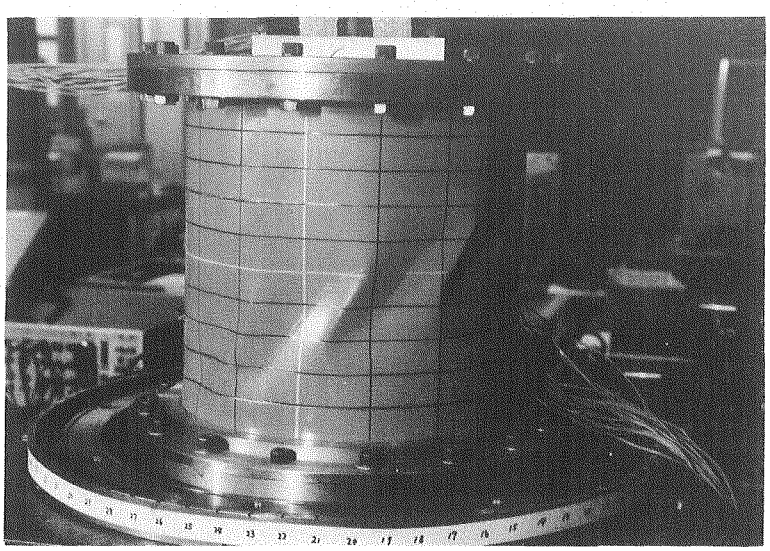

Photo 2. Shear Buckling Mode (IV-S4)

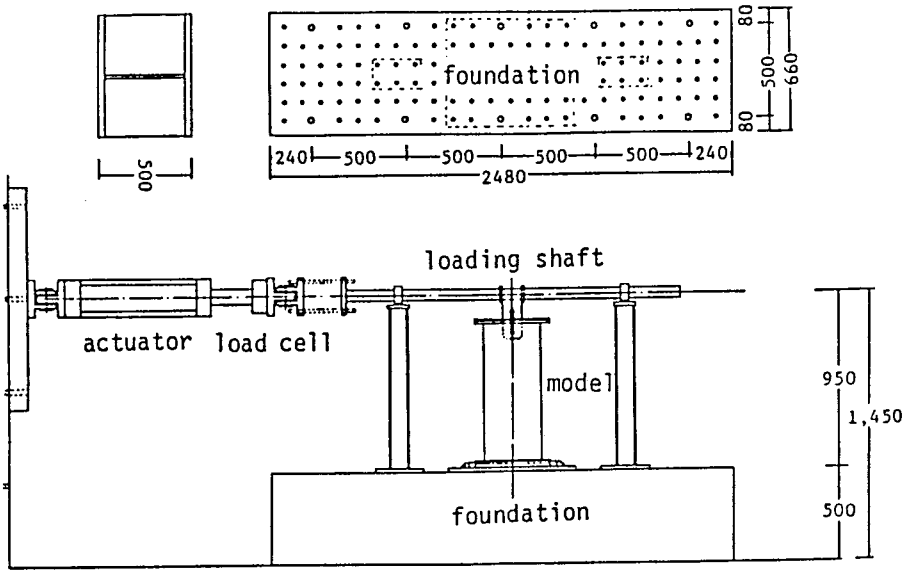

Fig.1. Test Set-up

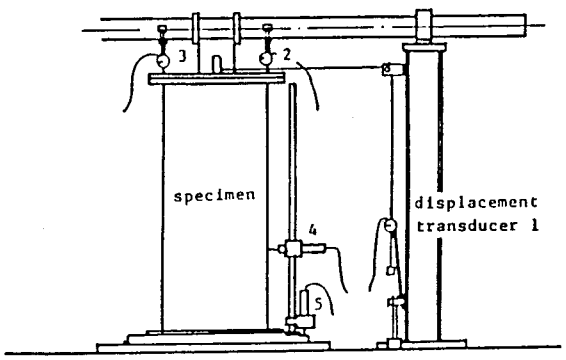

Fig.2. Device of Measurement

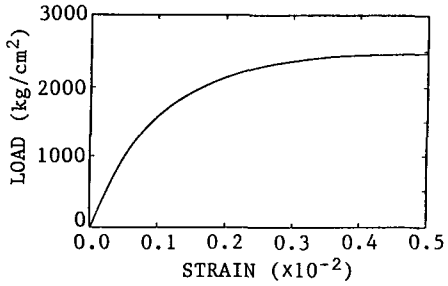

Fig.3. Stress-Strain Curve (steel)

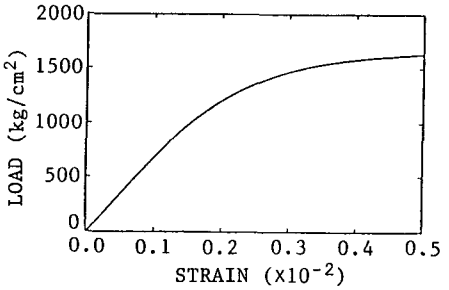

Fig.4. Stress-Strain Curve (alumini

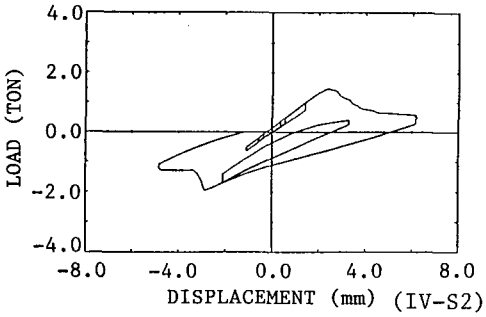

Fig.5. Load-Top Displacement Curve

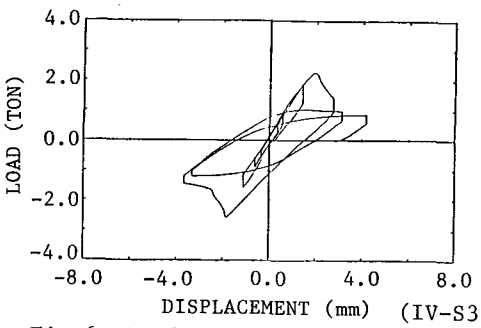

Fig.6. Load-Top Displacement Curve

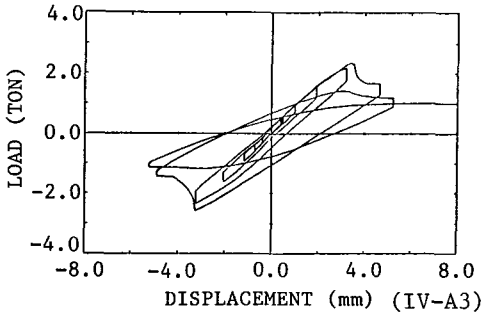

Fig.7. Load-Top Displacement Curve

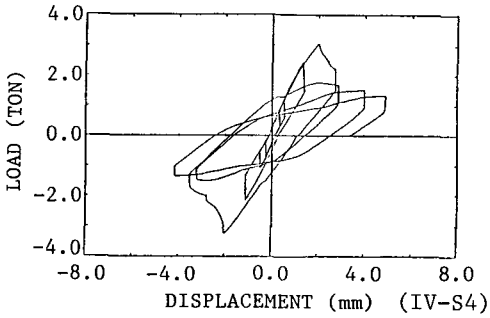

Fig.8. Load-Top Displacement Curve

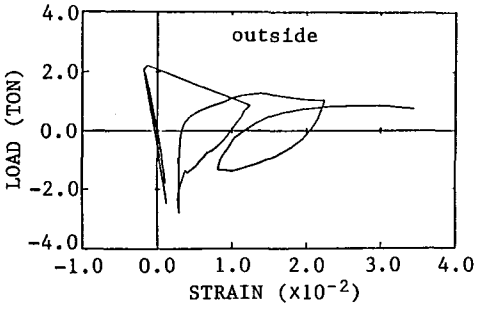

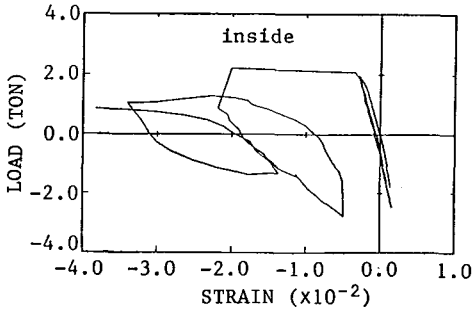

Fig.9. Load-Strain Curve (IV-A3, Gauge 1)

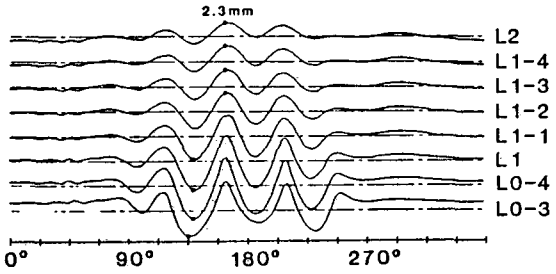

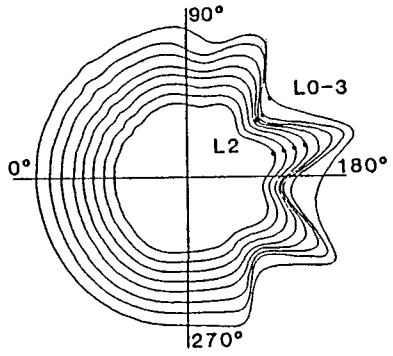

IV-A3 (step11)

Fig.10. Local Buckling Mode (IV-A3)

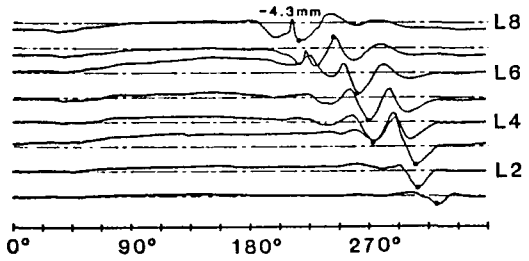

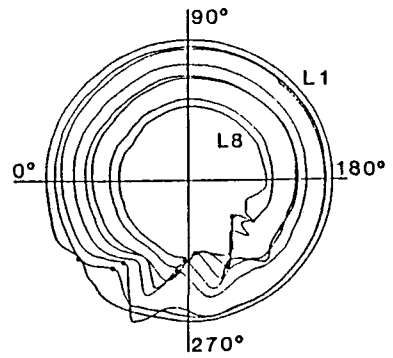

IV-S4 (step7)

Fig.11. Shear Buckling Mode (IV-S4)

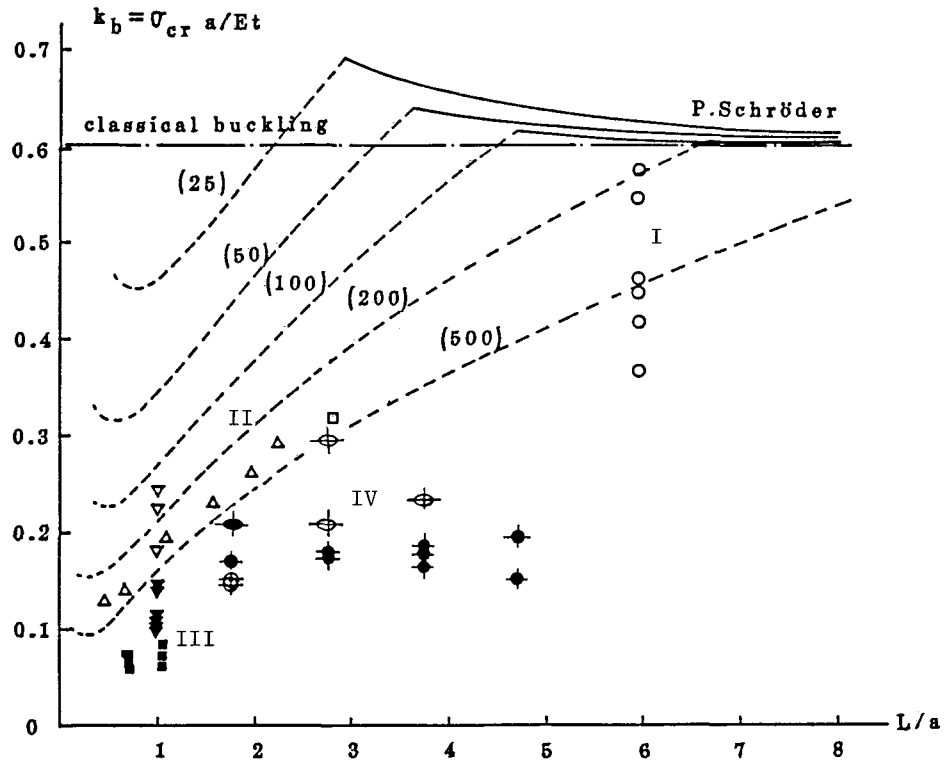

Present Results

: Local Buckling
: Shear Buckling

Ref.3

: Plastic Shear Buckling
: Elephant-foot Bulging

Elastic Buckling

○ : Ref.6 (a/t=250-750)
□ : Ref.7 (a/t=220)
△ : Ref.9 (a/t=405)
▽ : Ref.8 (a/t=200,300,400)

Plastic Buckling

▼ : Ref.8 (a/t=125,150,187)

Elephant-foot Bulging

■ : Ref.10 (Internal Pressure & Shear Force)

Fig. 12. Comparison of Test Results (Ref.11)